

Investigation of the influence of the subgrid-scale stress on non-intrusive spatial pressure measurement using an isotropic turbulence database

Xiaofeng Liu¹, Seth Siddle-Mitchel¹, Rachel Rybarczyk¹ and Joseph Katz²

¹ Department of Aerospace Engineering, San Diego State University, San Diego, California, U.S.A.
Xiaofeng.Liu@mail.sdsu.edu

² Department of Mechanical Engineering, Johns Hopkins University, Baltimore, Maryland, U.S.A.

ABSTRACT

The instantaneous pressure distribution in a turbulent flow field can be measured non-intrusively by integrating the measured material acceleration using particle image velocimetry (PIV). However, due to the finite spatial resolution of the measurement, the pressure reconstructed from PIV is actually subjected to the effect of spatial filtering. Consequently, the reconstructed pressure is effectively imbedded with the contribution of the sub-grid scale (SGS) stress, which is a term appearing in the filtered Navier-Stokes equation. To quantify the effect of the SGS stress on non-intrusive spatial pressure measurement, we use box filtering to filter three dimensional velocity components in a time-varying isotropic turbulence flow field available to public from the John Hopkins University Turbulence Database (JHTDB). Preliminary results show that the random error in the reconstructed instantaneous pressure caused by the SGS stress is about 4.4% of the r.m.s. fluctuation of the filtered isotropic pressure. Correction using similarity SGS stress modeling reduces the error to 2.1%.

MOTIVATION AND BACKGROUND

The instantaneous pressure distribution in an incompressible turbulent flow field can be measured non-intrusively by direct integration of the measured material acceleration, which constitutes the dominant contributor to pressure gradient for flow at high Reynolds number, as demonstrated by Liu and Katz [1-3], Joshi *et al.*[4], van Oudheusden [5] and Ragni *et al.* [6], to name a few. In addition, the pressure distribution can also be obtained by solving the Poisson equation, as shown in Violato *et al.* [7], and de Kat and van Oudheusden [8]. Review and comparison of the two pressure reconstruction approaches can be found in Charonko *et al.* [9] and van Oudheusden [10]. However, due to technical constraints, the spatial resolution of digital PIV is usually at least one or two orders of magnitude larger than the smallest turbulence length scale, i.e., the Kolmogorov length scale of the turbulent flow field, depending on Reynolds number. The resolution issue becomes even more prominent for tomographic PIV, as its resolution is usually coarser than that of planar PIV. Because of the finite spatial resolution, the pressure reconstructed from PIV is actually subjected to the effect of spatial filtering. Consequently, the reconstructed pressure is effectively imbedded with the contribution of the sub-grid scale (SGS) stress, which is a term appearing in the filtered Navier-Stokes equation as a result of the spatial filtering imposed by the finite resolution of the measurement.

To quantify the effect of the SGS stress on the accuracy of the non-intrusive spatial pressure measurement, we use box filtering to filter pressure as well as the three dimensional velocity components of a directly simulated isotropic turbulence flow field available to public from the John Hopkins University Turbulence Database (JHTDB) (Li *et al* [11] and Perlman *et al* [12]). As a way to simulate the pressure measurement process, we then apply the material acceleration calculation and pressure reconstruction procedures introduced in Liu and Katz ([1] and [3]) to obtain the pressure distribution. The reconstructed pressure, with and without the incorporation of the sub-grid scale stress, is compared with the pressure filtered directly from the DNS database, thus enabling quantification of the SGS stress influence on the reconstructed pressure.

To compensate the SGS stress influence, the SGS stress term calculated using the similarity model (Meneveau and Katz [13]) is incorporated in the pressure reconstruction process based on the filtered velocity data. The effectiveness of the compensation is then gauged by comparison with the filtered DNS pressure.

In the following sections of the paper, we start with a brief introduction of the John Hopkins University Turbulence Database (JHTDB). Subsequently, the methodology for investigation of the sub-grid scale stress influence of the pressure measurement is elaborated. After that, detailed results of the investigation will be presented and discussed. The paper will be concluded with a brief summary of the research findings together with a disclosure of the future research plan on this subject.

JHU ISOTROPIC TURBULENCE DATABASE

As mentioned earlier in the introduction, we use a fully resolved time-varying isotropic turbulence database available to public from the John Hopkins University (JHTDB) to quantify the effect of the SGS stress on non-intrusive spatial pressure measurement. The dataset offered from JHTDB is generated by direct numerical simulation (DNS) of forced isotropic turbulence [11-12]. The simulation was performed on a three dimensional periodic grid with $1024 \times 1024 \times 1024$ nodal points using a pseudo-spectral method for solving the Navier-Stokes equations. Fluctuation energy of the isotropic flow field at low wave number is injected at each step of simulation to maintain steady state conditions. The injection keeps constant energy in modes with wave-numbers less than or equal to 2. The database provides 1,024 instantaneous realizations in a $2\pi \times 2\pi \times 2\pi$ domain, with the 3 components of the velocity and the pressure fully-resolved, both temporally and spatially. The simulation time-step is 0.0002, and the time interval between stored samples in the database is 0.002, which is smaller than the Kolmogorov time scale of 0.0446, thus rendering fully-resolved temporal scales for the simulated isotropic turbulence. The grid size is 0.00614, which is on the same order of the Kolmogorov length scale of 0.00287. Figure 1 shows the pressure distribution in three adjacent planes selected from the DNS database.

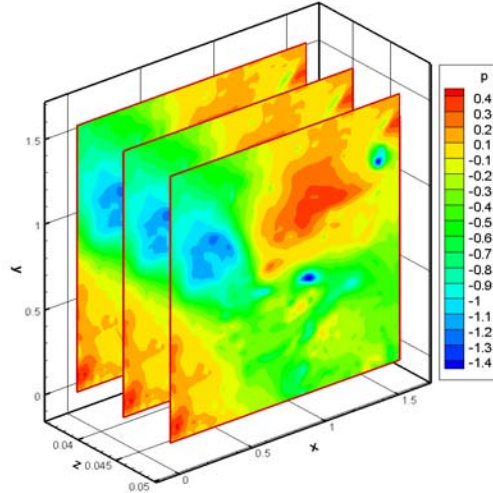


Figure 1. Three adjacent planes selected from the DNS cube.

GOVERNING EQUATION

The forced isotropic turbulence obtained by DNS is governed by the following momentum equation

$$\frac{\partial u_i}{\partial t} + u_j \frac{\partial u_i}{\partial x_j} = -\frac{\partial}{\partial x_j} \left[\frac{p}{\rho} \delta_{ij} \right] + \nu \frac{\partial^2 u_i}{\partial x_j^2} + f \quad (1)$$

where u_i denotes the i -th velocity component, p the pressure and f the forcing term. Correspondingly, the filtered momentum equation takes the form

$$\frac{\partial \tilde{u}_i}{\partial t} + \tilde{u}_j \frac{\partial \tilde{u}_i}{\partial x_j} = -\frac{\partial}{\partial x_j} \left[\frac{\tilde{p}}{\rho} \delta_{ij} + \tau_{ij} \right] + \nu \frac{\partial^2 \tilde{u}_i}{\partial x_j^2} + \tilde{f} \quad (2)$$

where “ \sim ” denotes filtering at a filter size of Δ . The sub-grid scale stress τ_{ij} is defined as

$$\tau_{ij} = \widetilde{u_i u_j} - \widetilde{u}_i \widetilde{u}_j \quad (3)$$

In equation (2), $\frac{\partial \widetilde{u}_i}{\partial t} + \widetilde{u}_j \frac{\partial \widetilde{u}_i}{\partial x_j}$ represents the material acceleration term, $-\frac{\partial}{\partial x_j} \left[\frac{\widetilde{p}}{\rho} \delta_{ij} \right]$ the pressure gradient term, $-\frac{\partial \tau_{ij}}{\partial x_j}$ the SGS stress term, $\nu \frac{\partial^2 \widetilde{u}_i}{\partial x_j^2}$ the viscous term, and \widetilde{f} the forcing term.

METHOD OF INVESTIGATION

As a preliminary effort of the investigation, a series of consecutive realizations of a sample volume with $256 \times 256 \times 13$ grid nodal points have been selected from the DNS database for investigation, as illustrated in the pressure distribution plot shown in Figure 1. To simulate the PIV filtering effect, velocity components and pressure in this $256 \times 256 \times 13$ selected domain (denoted as Grid Level 0) is spatially filtered using a $5 \times 5 \times 5$ box filter with 50% planar overlap, reducing the data to a $126 \times 126 \times 5$ coarse domain (denoted as Grid Level 1). This $5 \times 5 \times 5$ box filter effectively reduces the data resolution to 4×0.00614 , i.e., about 8.6 times of the Kolmogorov length scale of the forced isotropic turbulence. Thus the data on Grid Level 1 can be roughly viewed as a representation of the resolution level of PIV measurement. The resolved SGS stress on Grid Level 1, $\tau^{(1)}$, can be determined as

$$\tau_{ij}^{(1)} = \widetilde{u_i u_j} - \widetilde{u}_i \widetilde{u}_j \quad (4)$$

However, for real PIV data, the resolved SGS stress $\tau_{ij}^{(1)}$ is unknown. To estimate the SGS stress on the PIV resolution level, we have to resort to the SGS stress on a grid with coarser resolution, plus an appropriate scheme of the SGS stress modeling. To this end, data on Grid Level 1 is further filtered with a $3 \times 3 \times 3$ box filter to obtain SGS stress $\tau_{ij}^{(2)}$ on a $124 \times 124 \times 3$ grid, where $\tau_{ij}^{(2)}$ is defined as

$$\tau_{ij}^{(2)} = \widetilde{\widetilde{u}_i \widetilde{u}_j} - \widetilde{u}_i \widetilde{u}_j \quad (5)$$

where “ \approx ” represents the second time filtering over the Level 1 data. This quantity $\tau_{ij}^{(2)}$ can be used to substitute the unknown SGS stress $\tau^{(1)}$ for the PIV measurement, via appropriate SGS stress modeling. The similarity SGS stress modeling (Katz and Meneveau [13]) is invoked in this study because of its simplicity in use and its clear physical foundation. The similarity SGS stress modeling is based on the plausible assumption that the flow structure of the velocity field at the small scales (below the filter size Δ) is similar to that at larger scales (above Δ). This suggests that the SGS stress $\tau_{ij_model}^{(1)}$ on Grid Level 1 (PIV resolution level), must be similar to $\tau_{ij}^{(2)}$, a stress tensor constructed from the resolved velocity field. Thus, according the similarity SGS stress model [13], $\tau_{ij_model}^{(1)}$ can be modeled as

$$\tau_{ij_model}^{(1)} = c_{sim} \tau_{ij}^{(2)} \quad (6)$$

where c_{sim} is the modeling coefficient. In this study, c_{sim} is taken as 1.0. We use $\tau_{ij_model}^{(1)}$, determined from Equation (6), to investigate the effectiveness of SGS stress modeling on the accuracy improvement of the measured pressure. For the isotropic turbulence data obtained from the database, because the resolved velocity component (u , v , w) and pressure (p) are known, all terms in Equation (2), except the forcing term \widetilde{f} , can be evaluated directly for a given filtering size filter size Δ . The forcing term \widetilde{f} can be determined indirectly from the balance of Equation (2). These differential terms in Equation (2), and the linear combinations of the material acceleration with and without the addition of the viscous, forcing, and SGS stress terms as different level of approximation to the pressure gradient term, can be spatially integrated respectively

using the pressure reconstruction code developed by Liu and Katz [1-3]. The integrated results can then be compared with the filtered DNS pressure, which can be viewed as the “true pressure” that the PIV pressure measurement needs to capture at the PIV resolution level. In this way, the influence of the SGS term on the accuracy of the pressure measurement can be quantified. Meanwhile, influence of other terms of interest such as the viscous term on the pressure measurement can be evaluated as well.

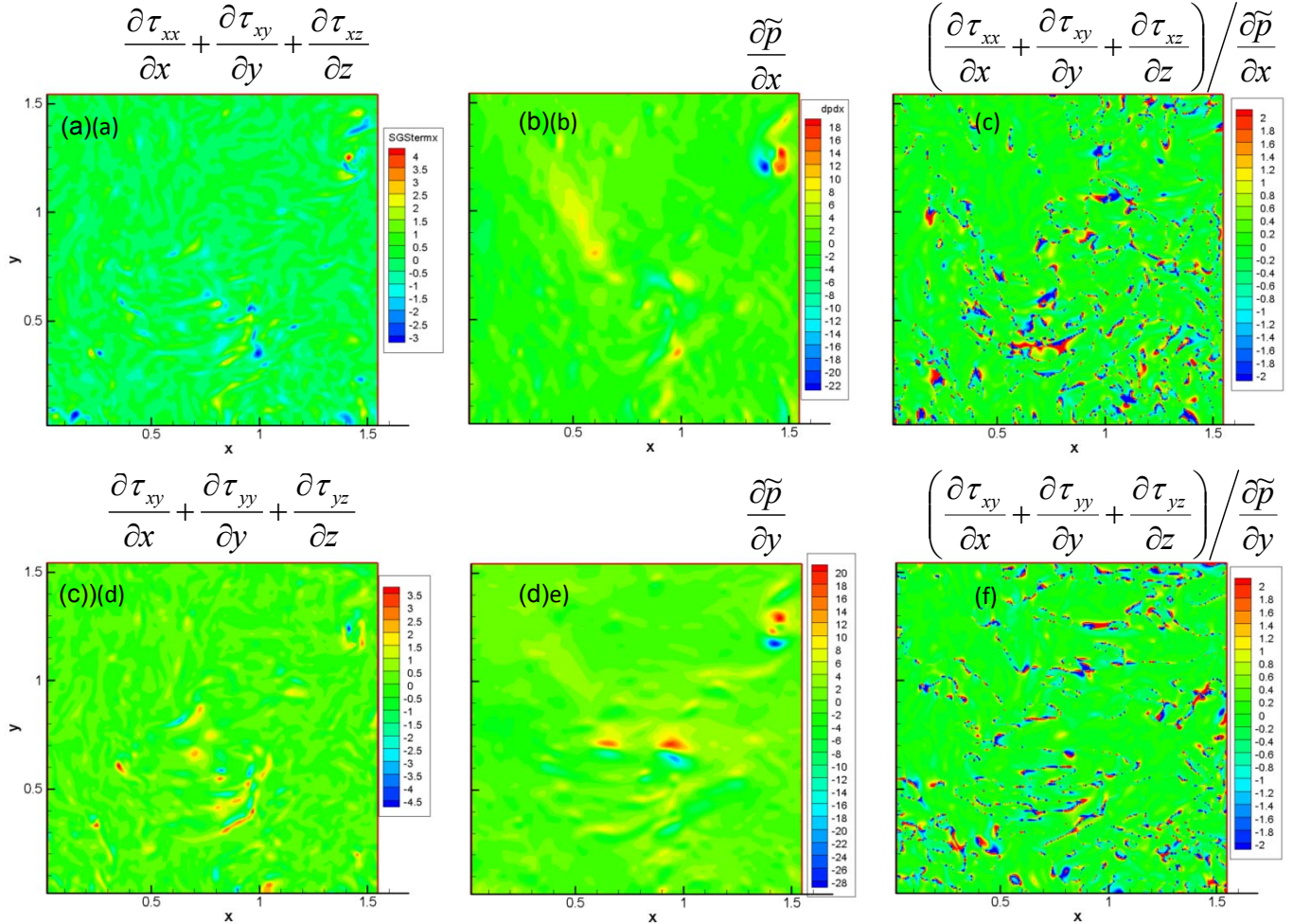


Figure 2. Comparison of the differential subgrid-scale stress term with the pressure gradients using the DNS isotropic turbulence data.

RESULTS AND DISCUSSION

The goal of this investigation is to determine the influence of the SGS stress on the accuracy of PIV pressure measurement. To begin with, we first examine the relative magnitude of the SGS stress tensor components in comparison with their corresponding pressure gradient terms. Figure 2 shows the distributions of the x - and y -components of the SGS stress term and the pressure gradients in Equation (2), as well as the distribution of the ratios between them, at the center plane of the $126 \times 126 \times 5$ coarse domain of Grid Level 1. As can be seen from Figure 2(a), (b), (d) and (e), overall the peak values of the SGS stress term are smaller than that of the corresponding pressure gradient. However, distributions of the ratio between the two quantities (Figure 2c and f) clearly show that at certain isolated regions the magnitude of sub-grid scale stress is considerably larger than that of the pressure gradient components. This qualitative understanding is further confirmed from the probability density function (pdf) distributions and the associated statistics of these two types of terms, as shown in Figure 3 and Table 1, respectively.

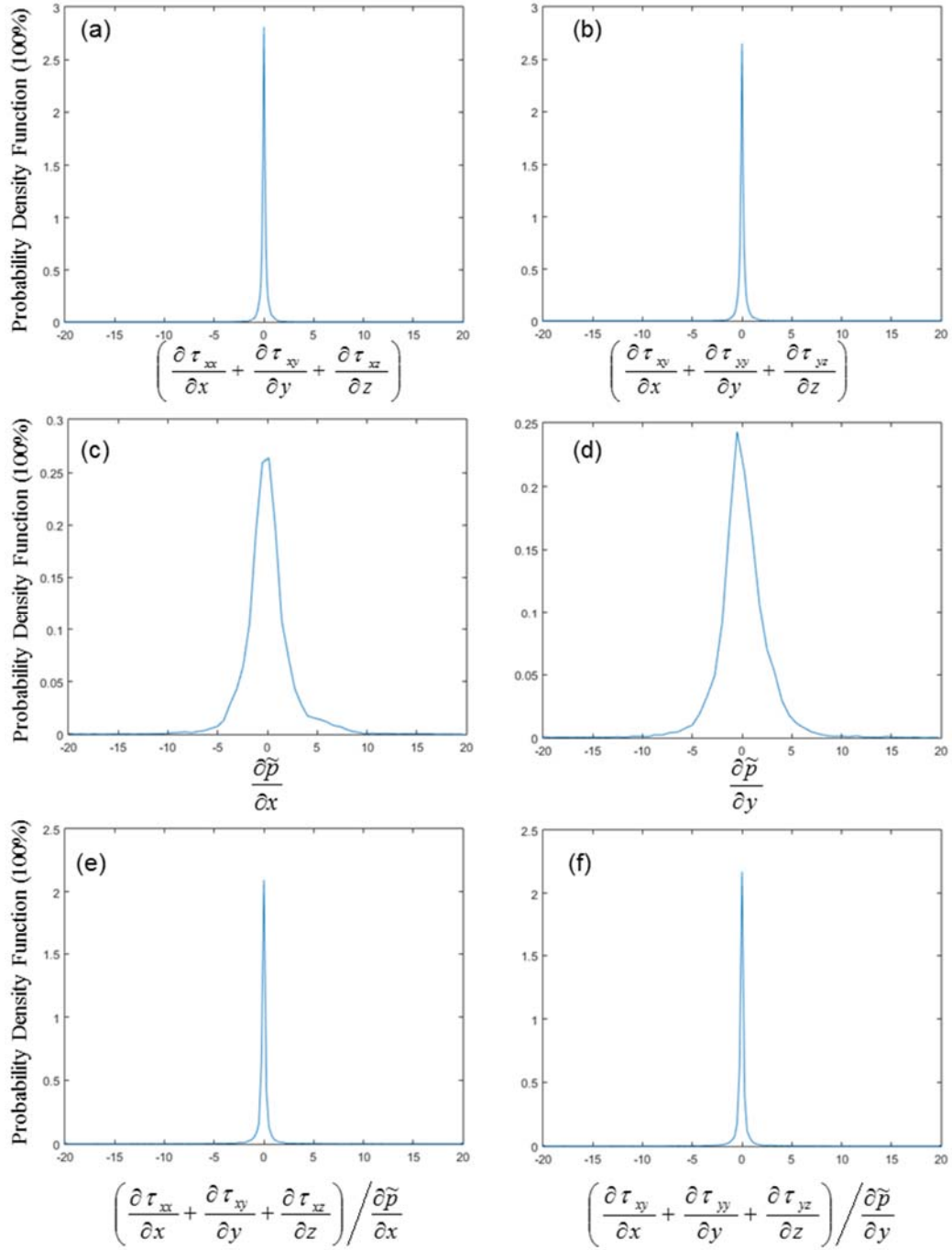


Figure 3. Probability density functions for the SGS stress term, the pressure gradients and their ratios at the center plane of the $126 \times 126 \times 5$ domain of Grid Level 1.

Table 1. Statistics of the SGS stress term, the pressure gradients and their ratios at the at the center plane of the 126×126×5 coarse domain of Grid Level 1.

	Mean	Standard Deviation, σ	Kurtosis, k	Kurtosis/ Standard Deviation, k/σ
$\rho \left(\frac{\partial \tau_{xx}}{\partial x} + \frac{\partial \tau_{xy}}{\partial y} + \frac{\partial \tau_{xz}}{\partial z} \right)$	9.826E-05	0.3654	13.7276	37.6
$\rho \left(\frac{\partial \tau_{xy}}{\partial x} + \frac{\partial \tau_{yy}}{\partial y} + \frac{\partial \tau_{yz}}{\partial z} \right)$	8.065E-3	0.3999	14.8162	37.1
$\frac{\partial \tilde{p}}{\partial x}$	2.658E-2	2.4281	12.0760	5.0
$\frac{\partial \tilde{p}}{\partial y}$	6.043E-2	2.7032	14.2552	5.3
$\rho \left(\frac{\partial \tau_{xx}}{\partial x} + \frac{\partial \tau_{xy}}{\partial y} + \frac{\partial \tau_{xz}}{\partial z} \right) / \frac{\partial \tilde{p}}{\partial x}$	0.1151	24.9153	9024.7	362.2
$\rho \left(\frac{\partial \tau_{xy}}{\partial x} + \frac{\partial \tau_{yy}}{\partial y} + \frac{\partial \tau_{yz}}{\partial z} \right) / \frac{\partial \tilde{p}}{\partial y}$	-0.1653	15.3343	13290.8	866.7

As shown clearly in Figure 3 and Table 1, all pdf profiles of these quantities are very close to be symmetric with respect to their almost zero mean values. However, the pdf distributions of both the x and y components of the SGS stress differential terms (Figure 3a and b) are strongly “outlier”-prone, as evidenced by their high kurtosis numbers ($\sim 37\sigma$, Table 1), indicating that their pdf profile shape is significantly deviated from that of the Gaussian distribution, for which the kurtosis value is 3σ . In contrast, the pdf profiles of the pressure gradient terms (Figure 3c and d), with a kurtosis value of about 5σ (Table 1), do not deviate very much from the Gaussian distribution. Examination of the pdf profiles shown in Figure 3(e) and (f) as well as the corresponding data in Table 1 finds that for ratio between the SGS stress differential term and the pressure gradient, the “outlier”-prone trend, apparently inherent from the SGS stress differential terms, is amplified to a remarkable level of $360 - 870\sigma$. This is in agreement with the plots shown in Figure 2(c) and (f) where at certain locations in the filtered flow field, the SGS stress differential terms have a dominant value that dwarfs the pressure gradient. This observation suggests that the neglect of the SGS stress term in the pressure reconstruction process may not be appropriate, because the local error in pressure gradient evaluation may have a global effect on the pressure distribution in the entire flow field. To quantify the influence of the SGS stress term on the accuracy of the reconstructed pressure, we resort to comparisons of the integral results of the different terms that constitutes Equation (2).

Figure 4 shows comparisons of the integral results of the viscous, forcing, SGS stress, and material acceleration terms with the filtered pressure at Grid Level 1 as well as the unfiltered DNS pressure. The integration is achieved using the pressure reconstructed code developed by Liu and Katz [1-3] based on *circular virtual boundary, omni-directional integration method*. The forcing term is obtained from the balance of Equation (2) as

$$\iint_{x-y \text{ plane}} \tilde{f} = \iint_{x-y \text{ plane}} \left(\frac{\partial \tilde{u}_i}{\partial t} + \tilde{u}_j \frac{\partial \tilde{u}_i}{\partial x_j} + \frac{\partial}{\partial x_j} \left[\frac{\tilde{p}}{\rho} \delta_{ij} + \tau_{ij} \right] - \nu \frac{\partial^2 \tilde{u}_i}{\partial x_j^2} \right) \quad (7)$$

As shown in Figure 4, at the Grid level 1 resolution, the peak values of the viscous term integral are one order of magnitude

smaller than that of the filtered pressure. In contrast, the peak values for the integrals of forcing, SGS stress and material acceleration terms are on the same order as that of the filtered pressure. As expected, the material acceleration is the dominant term in the filtered momentum equation that is balanced by the pressure gradient, as evidenced by their similar distribution patterns shown in Figure 4(d) and (e). However, as other significant contributors such as the forcing and the SGS stress terms not accounted for, the integral results of the material acceleration itself exhibits apparently deviation in magnitude from its filtered pressure counterparts, although their pattern of distributions are similar.

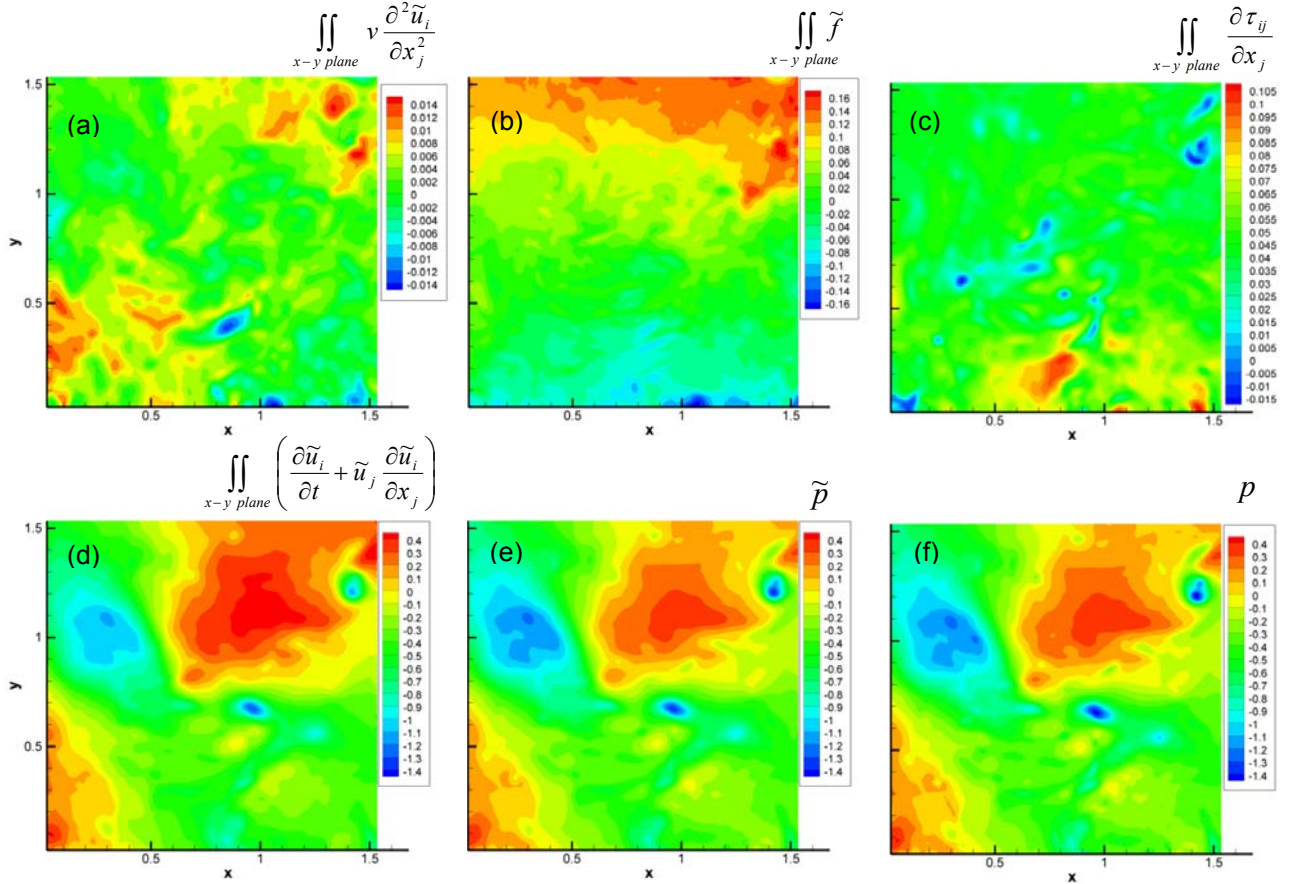


Figure 4. Comparison of the integral results of (a) viscous, (b) forcing, (c) SGS stress, and (d) material acceleration terms with (e) the filtered pressure and (f) the DNS pressure.

To gauge the effect of the different levels of approximation of the pressure gradient on the accuracy of pressure reconstruction, and to evaluate the effect of similarity modeling on compensation of the errors due to lack of resolved SGS stress, we define the following error quantities, with the filtered the pressure \tilde{p} treated as the “true value” for comparison:

$$\varepsilon_1 = \rho \iint_{x-y \text{ plane}} \left(\underbrace{\frac{\partial \tilde{u}_i}{\partial t} + \tilde{u}_j \frac{\partial \tilde{u}_i}{\partial x_j}}_{\text{Material Acceleration}} + \underbrace{\frac{\partial \tau_{ij}}{\partial x_j}}_{\text{SGS Stress}} - \underbrace{v \frac{\partial^2 \tilde{u}_i}{\partial x_j^2}}_{\text{Viscous}} - \underbrace{\tilde{f}}_{\text{Forcing}} \right) - \underbrace{\tilde{p}}_{\text{Filtered Pressure}} \quad (8)$$

$$\varepsilon_2 = \rho \iint_{x-y \text{ plane}} \left(\underbrace{\frac{\partial \tilde{u}_i}{\partial t} + \tilde{u}_j \frac{\partial \tilde{u}_i}{\partial x_j}}_{\text{Material Acceleration}} + \underbrace{\frac{\partial \tau_{ij}}{\partial x_j}}_{\text{SGS Stress}} - \underbrace{\tilde{f}}_{\text{Forcing}} \right) - \tilde{p} \quad \text{Filtered Pressure} \quad (9)$$

$$\varepsilon_3 = \rho \iint_{x-y \text{ plane}} \left(\underbrace{\frac{\partial \tilde{u}_i}{\partial t} + \tilde{u}_j \frac{\partial \tilde{u}_i}{\partial x_j}}_{\text{Material Acceleration}} - \underbrace{\nu \frac{\partial^2 \tilde{u}_i}{\partial x_j^2}}_{\text{Viscous}} - \underbrace{\tilde{f}}_{\text{Forcing}} \right) - \tilde{p} \quad \text{Filtered Pressure} \quad (10)$$

$$\varepsilon_4 = \rho \iint_{x-y \text{ plane}} \left(\underbrace{\frac{\partial \tilde{u}_i}{\partial t} + \tilde{u}_j \frac{\partial \tilde{u}_i}{\partial x_j}}_{\text{Material Acceleration}} + \underbrace{\frac{\partial \tau_{ij}^{(1)} \text{ - model}}{\partial x_j}}_{\text{Modeled SGS Stress}} - \underbrace{\nu \frac{\partial^2 \tilde{u}_i}{\partial x_j^2}}_{\text{Viscous}} - \underbrace{\tilde{f}}_{\text{Forcing}} \right) - \tilde{p} \quad \text{Filtered Pressure} \quad (11)$$

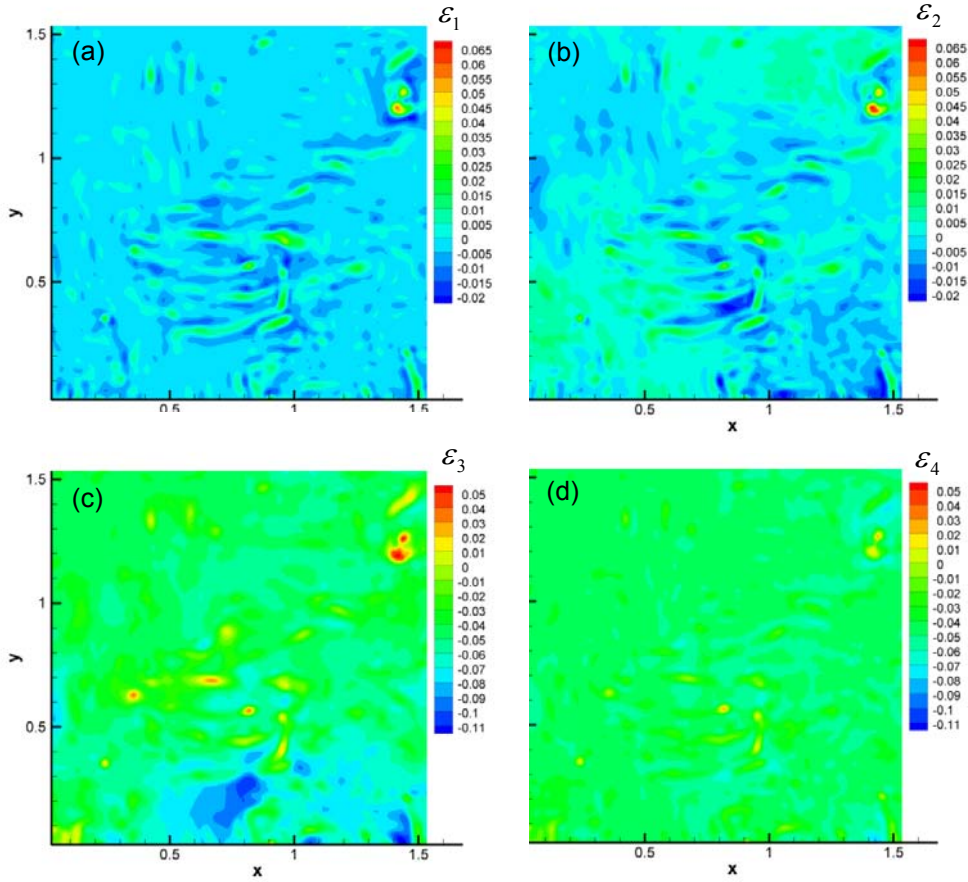


Figure 5. Comparison of the pressure differences between the reconstructed pressure at different levels of approximation and the filtered pressure \tilde{p} . (a), all terms accounted for. (b), viscous term only is neglected. (c), SGS stress term only is neglected and (d), SGS stress term is substituted with the modeled SGS stress based on similarity modeling.

As evident in the above definition, ε_1 represents the error of the integral in which all terms including material acceleration, SGS stress, viscous and forcing are accounted for to approximate the filtered pressure gradient. The filtered pressure \tilde{p} represents the true pressure value that the PIV measurement aims to capture. In contrast, ε_2 is used to examine the error due to the omission of the viscous term, while ε_3 to examine the effect of the neglect of the SGS term, and ε_4 to examine the effect of the SGS stress term being substituted with the modeled SGS stress, i.e., $\tau_{ij_model}^{(1)} = c_{sim} \tau_{ij}^{(2)} = \tau_{ij}^{(2)}$, where c_{sim} being taken as 1.0 in this study.

The distributions of the above errors are shown in Figure 5. Since all relevant terms have been accounted for, the error ε_1 shown in Figure 5(a) actually represents the lowest level of error that the reconstructed pressure can achieve, thus it is used as a base for comparison. The contributing sources to ε_1 mainly include a variety of numerical errors accumulated from different steps on the calculation procedures before obtaining the final integrals. The error ε_2 shown in Figure 5(b) indicates that the omission of the viscous term does not result in a noticeable increase in the error, in comparison with Figure 5(a). However, the neglect of the SGS stress term, as shown in Figure 5(c), results in a significant error increase in comparison with ε_1 . Using similarity model to substitute the unknown SGS stress obviously improves the situation, as demonstrated clearly in Figure 5(d).

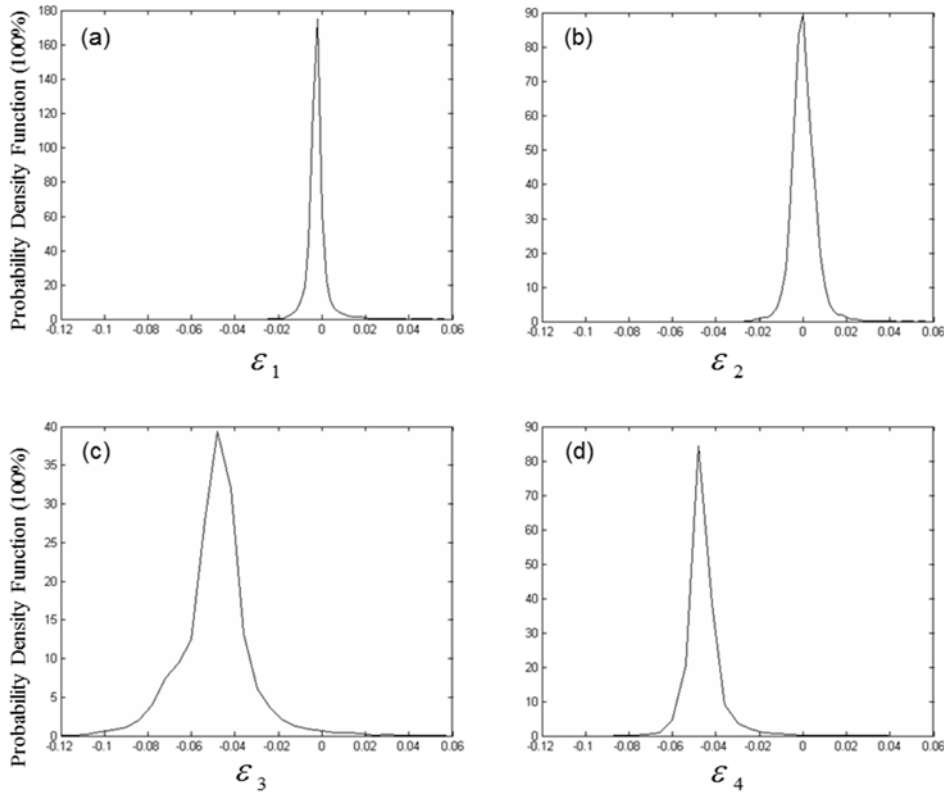


Figure 6 Probability density function of the differences between the reconstructed pressure at different levels of approximation and the filtered pressure \tilde{p} . (a), all terms accounted for. (b), viscous term neglected. (c), SGS stress term neglected and (d), SGS stress is substituted with the modeled SGS stress based on similarity modeling.

To further quantify these errors, pdf plots of these errors and their related statistics based on a total of five instantaneous realization samples are presented in Figure 6 and Table 2, respectively. The standard deviation of the fluctuating filtered pressure $\sigma_{\tilde{p}}$ (with an absolute value of 0.363) is used to gauge (normalize) the statistics. As the statistics in Table 2 reveals,

the neglect of the viscous term (ε_2) will not change much about the error statistics compared to that of ε_1 . This is in agreement with the comparison of Figure 5 (a) and (b). Actually the error due to the neglect of the viscous term is on the same order of the measurement error itself. Again, however, the neglect of the SGS stress term results in a significant increase in both the bias error (i.e., mean value of error normalized by $\sigma_{\tilde{p}}$) from -0.9% of the base case to -14.4% and the random error (i.e., standard deviation of error normalized by $\sigma_{\tilde{p}}$) from 1.3% to 4.4%. Similarity modeling using Grid Level 2 approximation to substitute the unknown SGS stress improves the situation by reducing the magnitude of bias error to 14.0%, and random error to 2.1%, as can be seen in Table 2. Please note that in PIV pressure measurement, this bias error may be corrected by offset of the measured mean pressure using a reference pressure.

Table 2. Statistics of the pressure differences.

	All terms accounted for, ε_1	Viscous term neglected, ε_2	SGS stress term neglected, ε_3	SGS stress based on similarity modeling, ε_4
Mean / $\sigma_{\tilde{p}}$	-0.009	-0.002	-0.144	-0.140
Standard Deviation / $\sigma_{\tilde{p}}$	0.013	0.016	0.044	0.021

Note: $\sigma_{\tilde{p}}=0.363$

CONCLUSIONS AND FUTURE WORK

The effect of the SGS stress on the accuracy of the non-intrusive spatial pressure measurement is investigated using data from a directly simulated isotropic turbulence flow field available to public at the John Hopkins University Turbulence Database (JHTDB).

Examination of the relative magnitude of the SGS stress tensor components against their corresponding pressure gradient terms shows that although at most area the magnitude of the SGS stress tensor is less than that of the pressure gradient, at certain locations in the flow field, the SGS stress differential terms may have a dominant value that dwarfs the pressure gradient, suggesting the neglect of the SGS stress term in the pressure reconstruction process may not be appropriate.

Comparison of the reconstructed pressure at different levels of pressure gradient approximation with the filtered pressure \tilde{p} shows that the neglect of the viscous term results in a negligible changes in the reconstructed pressure, because the error due to the neglect of the viscous term is on the same order of the measurement error itself. However, as a contrast, the neglect of the SGS stress term results in a significant increase in both the bias error the random error, suggesting the SGS term must be accounted for in the PIV pressure measurement. Correction using similarity SGS modeling reduces the random error from 4.4% to 2.1%, confirming the benefit of the error compensation method.

As for the ongoing and future work, a new set of analysis based on a more realistic first level filter size of $17 \times 17 \times 17$ is underway. In addition to using the isotropic turbulence database, the DNS channel flow data available at JHTDB will also be used to examine the SGS stress effect on pressure reconstruction in wall-bounded turbulent shear flow.

Acknowledgement

This project is funded by the San Diego State University Research Foundation. The help from Mr. Yunke Yang, Dr. Zuoli Xiao, Dr. Minping Wan, Dr. Huidan Yu and Prof. Meneveau in retrieving the isotropic turbulence data from the JHU database is gratefully acknowledged.

REFERENCES

- [1] Liu X and Katz J, 2006, “Instantaneous pressure and material acceleration measurements using a four exposure PIV system” *Experiments in Fluids*, Vol. 41, No. 2, 227-240.
- [2] Liu X and Katz J, 2008, “Cavitation phenomena occurring due to interaction of shear layer vortices with the trailing corner of a 2D open cavity”, *Physics of Fluids*, 20, 041702, DOI:10.1063/1.2897320..
- [3] Liu X and Katz J, 2013, “Vortex-corner interactions in a cavity shear layer elucidated by time resolved measurements of the pressure field”, *Journal of Fluid Mechanics*, Vol. 728, pp 417-457. DOI: 10.1017/jfm.2013.275.
- [4] Joshi, P., Liu, X. and Katz, J., Effect of mean and fluctuating pressure gradients on boundary layer turbulence, *Journal of Fluid Mechanics*, Vol. 748, June 2014, pp. 36–84. DOI:10.1017/jfm.2014.147.
- [5] Van Oudheusden BW, 2008, “Principles and application of velocimetry-based planar pressure imaging in compressible flows with shocks”, *Exp. Fluids* 45, 657–674.
- [6] Ragni D, Ashok A, Van Oudheusden BW and Scarano F 2009 “Surface pressure and determination of a transonic aerofoil based on particle image velocimetry”, *Meas. Sci.* 20, 074005.
- [7] Violato D, Moore P and Scarano F, 2011, “Lagrangian and Eulerian pressure field evaluation of rod-airfoil flow from time-resolved tomographic PIV”. *Exp. Fluids* 50, 1057–1070.
- [8] De Kat R and Van Oudheusden BW, 2012, “Instantaneous planar pressure determination from PIV in turbulent flow”, *Exp Fluids* 52, 1089–1106.
- [9] Charonko JJ, King CV, Smith BL and Vlachos PP, 2010, “Assessment of pressure field calculations from particle image velocimetry measurements”, *Meas. Sci. Tech.* 21, 105401.
- [10] Van Oudheusden BW, 2013, “PIV-based pressure measurement”, *Measurement Science and Technology* 24 (3), 032001.
- [11] Li Y, Perlman E, Wan M, Yang Y, Meneveau C, Burns R, Chen S, Szalay A and Eyink G, 2008, “A public turbulence database cluster and applications to study Lagrangian evolution of velocity increments in turbulence”, *J of Turbulence* 9(31).
- [12] Perlman E, Burns R, Li Y and Meneveau C, 2007, “Data Exploration of Turbulence Simulations using a Database Cluster”, *Supercomputing SC07*, ACM, IEEE, 2007.
- [13] Meneveau C and Katz J, 2000, “Scale-invariance and turbulence models of large-eddy simulation”, *Annu. Rev. Fluid Mech.*, 2000.